JOURNAL OF SPACECRAFT AND ROCKETS
Vol. 34, No. 5, September–October 1997

Transient Potential Modification of Large Spacecraft Due to Electron Emissions

Sven G. Bilén,* Victor M. Agüero,† and Brian E. Gilchrist‡
University of Michigan, Ann Arbor, Michigan 48109
and
W. John Raitt§
Utah State University, Logan, Utah 84322

The transient potential response of a large spacecraft structure in low Earth orbit due to electron generator emissions has been investigated experimentally using the Tethered Satellite System on NASA's Space Shuttle and by equivalent-circuit-model simulations. The model simulations of this highly distributed and complex structure demonstrate that useful predictions of high-speed potential behavior and charging levels can be made. Our experimental results were obtained when an electron generator emitted pulses into the surrounding nighttime ionospheric plasma. Because of the surrounding plasma's low density, the electron generator modified the Shuttle's potential quickly and by several volts. Our experimental system measured the resulting voltage transients by selectively sampling the system voltage in high-speed bursts. The model simulations show that the transient potential response of the system is due to a combination of the system's electrical circuit and the modification of the Shuttle's potential due to the electron generator emissions. Computer simulations also were used to perform parametric studies of transient spacecraft potential modification for varying plasma densities, electron-beam currents, and electron collection areas. These results have implications for the use and simulation of electron generators that actively modify the potential of their host spacecraft.

Nomenclature

A_e = electron collection area, m^2
A_i = ion collection area, m^2
C_{orb} = Orbiter capacitance, F
C_{sat} = satellite sheath capacitance, F
I_{CS} = Orbiter capacitance discharge current, A
I_E = incident electron current, A
I_{eng} = current to engine bells, A
I_I = incident ion current, A
I_{ram} = ion ram current, A
I_{sat} = current to satellite, A
I_{tether} = tether current, A
J_{e0} = electron current density, A/m^2
J_{ir} = ion ram current density, A/m^2
k = Boltzmann's constant, 1.38×10^{-23} J/K
m_e = electron mass, 9.109×10^{-31} kg
n_e = plasma density, m^{-3}
n_i = ion density, m^{-3}
q = elementary charge magnitude, 1.602×10^{-19} C
R_{open} = Tethered Satellite System open-circuit load impedance, Ω
V_{CS} = voltage on Orbiter capacitance discharge current source, V
V_{eng} = voltage on engine bells, V
V_{sat} = voltage on satellite, V
v_s = spacecraft velocity with respect to flowing plasma, m/s
α_e = nondimensional electron sheath factor
α_i = nondimensional ion sheath factor
θ_e = electron temperature, eV
θ_i = ion ram energy, eV

Introduction

PREDICTING steady-state and transient spacecraft potentials remains of fundamental importance for a variety of scientific and technological applications because the charging of spacecraft, due to either natural processes or active emission of charge, can alter the performance of sensitive instruments as well as induce possibly damaging charging levels.[1] The potential of large spacecraft, especially those operating with exposed high-voltage systems such as the International Space Station, can be dramatically and rapidly modified due to a complex set of external and internal processes.[2] These processes are also of importance to electrodynamic tether systems for which active collection of current necessarily involves charging effects and transient switching responses.[3,4]

To date, several experimental systems have flown to examine these processes. These systems include the Cooperative High Altitude Rocket Gun Experiments (CHARGE-2) suborbital rocket flown in December 1985 (Ref. 5), the Space Power Experiments Aboard Rockets (SPEAR-1) suborbital rocket flown in December 1987 (Ref. 6), and the first Tethered Satellite System (TSS-1) orbital mission flown in August 1992. In their experimental systems, CHARGE-2 and SPEAR-1 applied differential biasing between different parts of the rocket systems to alter their platform potential; CHARGE-2 and TSS-1 also used an electron generator.[7]

With the exception of CHARGE-2, however, the spacecraft potential measurements made to date have been of relatively low temporal resolution. Although CHARGE-2 did make high-speed (10 MHz) spacecraft potential measurements, they were taken in short, 100-μs bursts spaced approximately 1 s apart. With the Shuttle Electrodynamic Tether System (SETS) on TSS-1, we were able to sample vehicle potential at fairly high rates (32 kHz) for longer periods of time (1-s bursts). These measurements allowed us to develop a detailed model of the Orbiter–tether–satellite system and its interaction with the local plasma environment. This model allows us to predict the response of the TSS system to quickly changing potential modifications. Note that the ability to make these Orbiter potential measurements was facilitated by using the tethered satellite as a remote plasma reference.[8]

Received Nov. 26, 1996; revision received April 2, 1997; accepted for publication April 21, 1997.

*Graduate Student Research Assistant, Radiation Laboratory, Electrical Engineering and Computer Science Department, and Space Physics Research Laboratory, Atmospheric, Oceanic, and Space Sciences Department. Student Member AIAA.

†Visiting Scholar, Space, Telecommunications, and Radioscience Laboratory, Department of Electrical Engineering. Member AIAA.

‡Assistant Professor, Radiation Laboratory, Electrical Engineering and Computer Science Department, and Space Physics Research Laboratory, Atmospheric, Oceanic, and Space Sciences Department. Member AIAA.

§Professor, Department of Physics. Member AIAA.

During TSS-1, we had the unique opportunity to study the system's steady-state and high-speed transient response to spacecraft potential changes. We provide first reports of the TSS transient response to the firing of its electron generator into the local low-density ionosphere. We have expanded the tether system model developed by Bilén et al.[4] to include a circuit model of the electron generator as well as a more accurate model of the plasma response at the Orbiter. The Bilén et al. model accounts for the variability and asymmetry seen in TSS-1 mission electrodynamic tether switching transients. These transients occurred when the TSS system switched from its current-measuring mode to its voltage-measuring mode. The observations used in the present analysis were made when TSS-1 was in its voltage-measuring mode and the electron generator was actively and quickly modifying the Orbiter potential.

The TSS-1 mission and SETS experiment system are introduced, and their operation is described. We then present the transient observations from the TSS-1 mission used in our analysis, describe the electrodynamic tether system transient model when flying through the ionosphere, and compare experimental results with model predictions.

TSS–SETS Experiment System

TSS-1 was a joint mission between NASA and ASI (Italian Space Agency) that flew onboard STS-46 in August 1992 (Refs. 3 and 9). TSS-1 deployed an electrically conductive, 1.6-m-diam Italian-built satellite to a distance of 267 m above the payload bay of the Space Shuttle *Atlantis*, which was at an altitude of approximately 296 km. The satellite was connected to the shuttle via an electrically conducting insulated wire, and the interaction of this wire with the Earth's magnetic field induced a potential across the tether reaching values near 60 V, which allowed tether currents approaching 30 mA.

Central to the results reported here is the SETS experiment that made high-resolution measurements of the induced tether potential using a high-impedance voltage monitor.[10] SETS also controlled current flow through the tether using switched loads and active electron-beam emissions. To measure I–V tether characteristics, the SETS experiment could selectively place resistive loads between the tether end and the Shuttle's electrical ground, allowing current to flow through the tether from the ionospheric plasma. The load connections were made with and without 1-keV electron-beam emissions from the SETS fast-pulsed electron generator (FPEG), which was connected to the Orbiter electrical ground. Because of the orbitally induced potential polarity, the TSS-1 satellite was typically biased to attract electrons to its conducting surfaces while the Orbiter either attracted ions to its main engine bells—its primary conducting surfaces—or emitted electrons via the FPEG.

In the present analysis, data from three SETS instruments were used: the dc tether voltage monitor (TVMDC), tether current monitor (TCM), and current mode monitor (CMM). The TVMDC is the primary measurement of tether potential and features 16-bit resolution, 360-Hz sampling rate, and three gain states: $\times 1$, $\times 10$, and $\times 100$. The TCM is a Hall-effect probe that makes no direct contact with the tether circuit. It has a 16-bit resolution and a sample rate of 24 Hz. The CMM is a dc coupled burst measurement of the tether potential applied to the load resistor bank and also has three gain states: $\times 1$, $\times 10$, and $\times 100$. It is an 8-bit digitizer (1-bit resolution: $\times 1$, 39.4 V; $\times 10$, 3.96 V; and $\times 100$, 0.397 V) with a programmable sample rate of up to 10^7 samples/s that can be used to capture transient events. During TSS-1, the CMM was filtered with a 12-kHz double-pole low-pass filter. The CMM signal is available only through a burst-mode channel that can handle up to 4 captures with a total of 32,000 samples each before downloading them in the telemetry stream. For the experiments discussed in the present analysis, the CMM measurements were made at $\times 10$ and $\times 100$ gains at a rate of 32 kHz. More information on these instruments can be found in Ref. 10.

The SETS FPEG was used to eject electrons from the Orbiter to study the TSS current balance and Orbiter charging in different ionospheric conditions and under different TCVM resistive loads. The FPEG has two independent gun assemblies, each capable of emitting 1-keV electrons with a beam current of 100 mA per assembly. Each gun assembly has a separate filament power supply, high-voltage power supply, and solid-state high-voltage switch. Beam emission is controlled by the high-voltage switch, which, when on, connects the filament directly to the high-voltage power supply. The FPEG electron beam can be pulsed at high rates because of the short, 100-ns rise and fall times of the high-voltage switch. The on and off times of the pulses can be programmed separately.[10,11] For the data reported here, the FPEG was commanded to fire one filament (100 mA) with an on and off time of 13.1 ms, giving a pulse frequency of 38.2 Hz. The beam heads are aimed 23 deg up from the Orbiter's $+y$ direction such that it fires over the starboard wing. Figure 1 shows the location of the FPEG in the Orbiter's cargo bay.

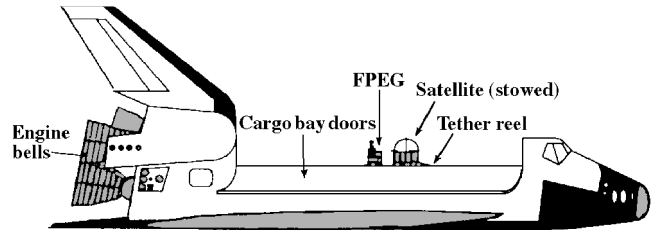

Fig. 1 TSS-1 showing the location of the satellite (stowed), tether reel, SETS FPEG, cargo bay doors, and engine bells.

The TSS tether deployer system consists of a large tether storage reel that is mechanically turned to wind tether on and off. This reel is a 121.9-cm-long, fiberglass-coated, hollow aluminum spindle that is 11.3 cm in diameter and has 96.5-cm aluminum flanges on each end.[12] Both the spindle and its flanges are electrically grounded to the Orbiter. Fully wound before satellite deployment, the system contains 22 km of insulated tether wrapped on the reel and can be considered electrically as an inductor of approximately 12 H with parasitic capacitances and resistances.[4]

Observations

The observations used in this analysis were chosen because they met four criteria: 1) The FPEG was placed in a pulsing mode rather than a dc firing mode, 2) the TSS system was in a region of low local plasma density, 3) the CMM captured high-speed voltage data, and 4) the CMM data were not limited by instrument resolution nor were they saturated. Two such observations met these criteria and are listed in Table 1. They occurred during one of the TSS-1 experiments called joint functional objective number 2 (JFO2, also called DEP1), of which there were a total of 98 performed. (A more detailed description and complete plots of JFO2 can be found elsewhere.[10]) More specifically, the events occurred during JFO2 step 2, which characterizes the FPEG's ability to support current flow through the tether system. In this step, FPEG beam emissions occur as each TCVM load resistor is switched in and then out individually. In addition, a quick SHUNT closure ($\approx$40 ms in length) occurs at the beginning of the step, and at this time the CMM captures data. For most of the JFO2 executions, the FPEG emitted a dc beam; however, there were seven executions during which the beam was pulsed instead at 38.2 Hz. Of these seven, five occurred in a region of low local plasma density such that the Orbiter potential could be quickly modified by the FPEG. Although the CMM captured high-speed data during these five, in only two were the CMM data not limited by instrument resolution, allowing rigorous analysis.

These two observations are shown in Figs. 2a and 2b, which show the Orbiter potential modification via the FPEG pulsing. Shown are the tether potential, tether current, load resistor in use, Greenwich Mean Time, and CMM captured transient response for the observations. The vertical dotted line is the time when the CMM burst data are collected. Also included is the simulated transient response, which is discussed later. Although the quick modification of the Orbiter potential can be seen in the tether potential measurement, which was collected with the 360-Hz sampling rate TCVM, the data are aliased and are not easily resolved. The CMM measurement, which was collected at 32 kHz, shows that the Orbiter potential is easily modified by the FPEG and also that a second-order ringing response is excited by this firing. This second-order ringing has been shown to be the pulse response of the TSS tether

deployer system,[13] which is similar to the pulse response of a transformer.[14]

To analyze these observations, we must know the local ionospheric plasma density around the Orbiter. Normally, direct density measurements were made by the Research on Electrodynamic Tether Effect's (RETE) Langmuir probe. At the time of these observations, however, no direct density measurement was available. Thus, we estimate it using the technique of Thompson et al.[15] Their approach requires that the Orbiter be moving with a supersonic velocity v_s with respect to the ambient ions. They then assume an effective ion collection area A_i of the Orbiter engine bells and state that the ion ram current I_{ram} collected to the uncharged Orbiter is equal to the tether current I_{tether} such that

$$n_e = \frac{I_{\text{tether}}}{A_i q v_s} \tag{1}$$

Because reasonable estimates of n_e from Eq. (1) require $I_{\text{tether}} = I_{\text{ram}}$, two conditions affecting I_{tether} must be satisfied: The FPEG must not be firing and I_{tether} must not be limited by tether resistance. To satisfy the first condition, we cannot use I_{tether} from JFO2 step 2 because the FPEG is firing. Step 3 of JFO2, however, follows the same switching sequence as step 2 but without FPEG emissions and, although separated by 140 s, a reasonable value of I_{tether}, and hence plasma density, can be obtained during step 3. The second condition—that I_{tether} not be limited by tether resistance—generally was met easily when TSS-1 flew through regions of low plasma density. Because both conditions can be met, Eq. (1) provides a reasonable estimate of plasma density for the observations reported here (involving low Orbiter charging and available tether emf of less than 10 V). Estimates are listed in Table 1. The conclusion that the observations during this time period took place in low plasma density conditions is corroborated by observations discussed by Oberhardt et al.[16] using the Shuttle Potential and Return Electron Experiment (SPREE).[17]

During the time of these observations, TSS was in its initial deployment phase and the orientation of the Shuttle was such that its engine bells were directed in the ram direction with its nose pitched down 37 deg, placing the payload bay into a deep wake. The satellite itself was in close proximity to the Shuttle and firing a neutral-gas thruster to propel it away from the Orbiter. However, the neutral-gas density in the payload bay was already sufficiently low to allow instruments with exposed high-voltage systems to be turned on safely. Further, simultaneous FPEG operations with certain Orbiter thruster firings were separately shown to enhance plasma density in the payload bay using the SPREE instrument.[16] If significant density enhancement had occurred during the observational period discussed here, spacecraft positive charging would have been reduced.

Table 1 Summary of TSS-1 JFO2 used in analysis

DEP1 event	Greenwich mean time, ddd/hhmm:ss	Burst-mode time, ddd/hhmm:ss	Estimated density, $\times 10^{10}$ m^{-3}	Tether length, m
30	217/2310:23	217/2312:05	3.2	25.9
31	217/2318:08	217/2319:50	5.2	44.7

Electrodynamic Tether System Model

We have expanded the model developed by Bilén et al.[4] to include a circuit model of the FPEG as well as a more complete electrical model of the Orbiter. Their model was used to account successfully for the ionosphere-induced variability and asymmetry seen in TSS-1 mission electrical transients—the transient case that occurred when the TSS system switched between its current-measuring mode and its voltage-measuring mode. When TSS-1 was in the current-measuring mode, a selectable load impedance (15 Ω, 25 kΩ, 250 kΩ, or 2.5 MΩ) was placed between the tether and the Orbiter, which allowed a measurable current to flow. In the voltage-measuring mode, TSS-1 was in a configuration in which only the high total impedance (≃35 MΩ) of the SETS and deployer core equipment (DCORE) voltage monitors was connected between the tether and the Orbiter end. In this case, negligible current flows along the tether and almost all of the voltage drop in the system occurs across this high-impedance load, allowing an accurate measurement of tether potential. The observations used in the present analysis were made when TSS-1 was in its voltage-measuring mode.

For our discussion, the expanded equivalent circuit model of TSS-1 is divided into six sections: 1) satellite, 2) electrodynamic tether, 3) tether reel, 4) SETS, 5) Orbiter, and 6) FPEG, as shown in Fig. 3. Because the first three have not been modified and are described in detail by Bilén et al.,[4] only a brief, qualitative overview for them is given here. The remaining three have been modified, and more rigorous descriptions are given. In our description, we begin

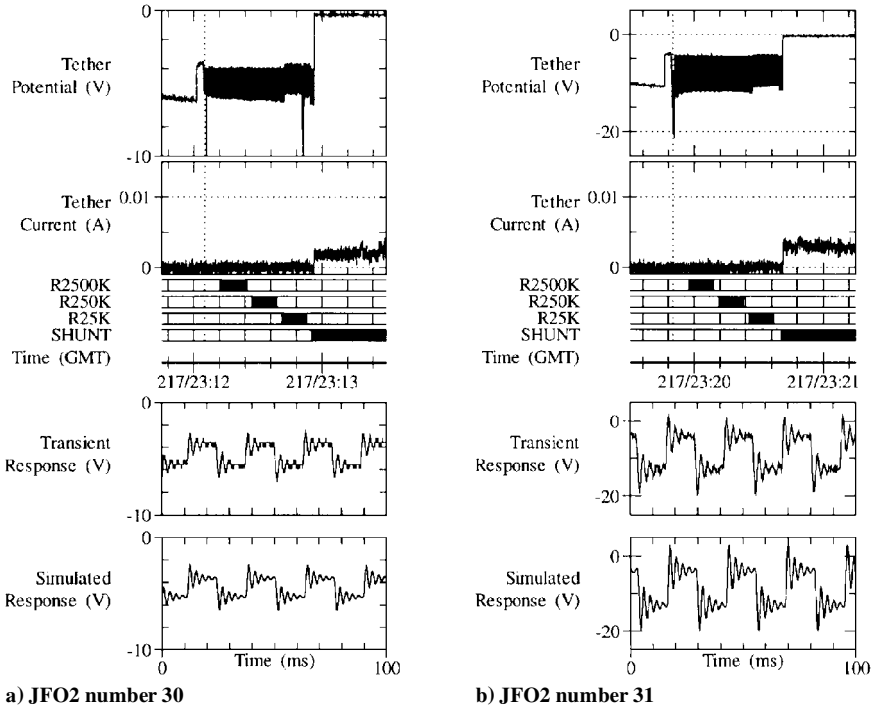

a) JFO2 number 30 **b) JFO2 number 31**

Fig. 2 Orbiter potential modification via electron generator pulsing.

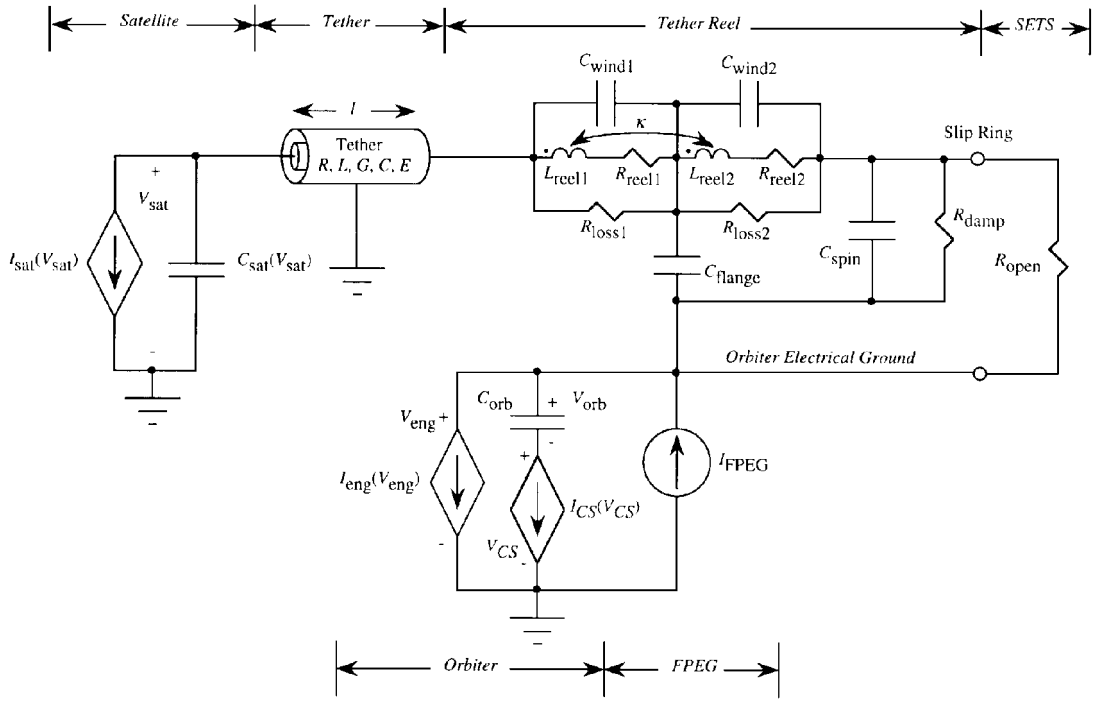

Fig. 3 Equivalent TSS-1 circuit model showing satellite, tether, tether reel, SETS, Orbiter, and FPEG sections.

with the Orbiter section because it is most important and move in a counterclockwise fashion through the remaining sections of Fig. 3. Note that the model described here is applicable to transient analyses, i.e., short timescales (tens of milliseconds or less). For longer timescales (hundreds to thousands of milliseconds), the reader is referred to other models such as that developed by Agüero.[8]

Orbiter Model

The Orbiter surfaces, i.e., its main engine bells and cargo bay doors (see Fig. 1), can be considered as probes that are immersed in the surrounding ionospheric plasma and, as such, have characteristic I–V responses or nonlinear conductances. To simulate these nonlinear conductances, each conductance is based on a physical current source model as developed by Brundin[18] and Garrett.[19] This source model assumes a low potential linear ion ram flux and electron current collection levels that remain close to or less than the thermal current capabilities of the Orbiter, which is appropriate for the cases studied here.

In the Orbiter model, two physical current sources are placed between the Orbiter electrical ground and the ionosphere. The first current source represents the interaction of the Orbiter's engine bells with the ionosphere. (Although there are other conducting surfaces, the Orbiter's primary conducting surfaces are the engine bells.) The current to the engine bells I_{eng} as a function of voltage V_{eng} with respect to the local plasma and neglecting magnetic, photoelectric, and secondary effects is given by

$$I_{eng}(V_{eng}) = I_I(V_{eng}) - I_E(V_{eng}) \tag{2}$$

For $V_{eng} \leq 0$, Eq. (2) can be written as

$$I_{eng}(V_{eng}) = A_i J_{ir}[1 - \alpha_i(V_{eng}/\theta_i)] + A_e J_{e0} \exp(V_{eng}/\theta_e) \tag{3}$$

where $J_{ir} = qn_i v_s$ when the ion thermal velocity is ignored and

$$J_{e0} = \left[qn_e \sqrt{\frac{k\theta_e(11{,}600\,\mathrm{K/eV})}{2\pi m_e}} \right]$$

For the first source, $A_i = A_e \approx 25\,\mathrm{m}^2$ based on TSS-1 data and represents the approximate effective collection area of the Orbiter,[15,20] although somewhat larger values for collection area also have been suggested.[21] The value A_i represents the approximate cross-sectional surface area presented to the flowing mesosonic ion flux and thus is dependent on the attitude of the Orbiter, that is, whether the engine bells are in the Orbiter's ram or wake. For the present observations, the engine bells were in the ram; therefore, the full value of A_i is used. Other values for TSS-1 are $v_s = 7.5$ km/s, $\theta_e \approx 0.2$ eV, and $\theta_i \approx 5$ eV.

The factor $(1 - \alpha_i V_{eng}/\theta_i)$ in Eq. (3), where $V_{eng} < 0$, represents a modification to the effective engine bell ram cross-sectional area A_i to account for an increase in the effective impact radius for ions due to an expanded plasma sheath. The ion sheath factor α_i is small if variation of engine bell potential has little or no effect on ion collection. In this case the ion current is exclusively due to ram ion flux. On the other hand, α_i is close to unity if engine bell potential variation strongly influences ion current collection. In this case, the total ion collection area includes the expanded plasma sheath. These two cases are analogous to the thin and thick sheaths described in Ref. 19. If the sheath is thin with respect to engine bell dimensions, then potential variations will have little effect on ion current collection, whereas if the sheath is thick, then the potential variation has a large effect on ion current collection. The ion sheath factor α_i was determined qualitatively from the computer simulations to be 0.1, approximating a thin sheath. This choice of α_i implies that the expanded sheath contribution is only a fraction of the ion collection when the effective collecting area of the engine bells for these low-charging-magnitude events is taken as 25 m^2 (as assumed by Thompson et al.[15]). Recent published work[8] provides an explanation for the reasonableness of this assumption by identifying in detail the current collection contributions to the charging balance for the range of negative charging events observed during TSS-1, the result being that the 25-m^2 area is a good average for the effective current collecting area of the Orbiter (including sheath contributions) when the Orbiter is charged to a magnitude in the range of the available emf for these events.

Note that, as written, Eq. (3) is strictly valid only for voltages $V_{eng} \leq 0$. To extend Eq. (3) to $V_{eng} > 0$, which is necessary because FPEG emissions charge the Orbiter positively, we specify an electron saturation region such that the exponential term does not increase indefinitely. We specified this region in our current source model as $(I_{eng})_{V_{eng}>0} = A_e J_{e0}(1 + \alpha_e V_{eng}/\theta_e)$, where $A_e J_{e0}$ represents the thermal electron current collected by the Orbiter's engine bells, which is allowed to grow as V_{eng} increases. The ion-current term becomes insignificant in the positive regime because the electron-current term dominates. With this addition, we obtain

an I–V response similar to the classic cylindrical Langmuir-probe I–V response.

The second current source, $I_{CS}(V_{CS})$, discharges the Orbiter capacitance C_{orb}, which is a physical capacitance resulting primarily from the layered dielectric coating on the Orbiter cargo bay doors.[22] For our analysis, we have assumed $A_i = A_e \approx 100$ m^2 for the case of I_{CS}. The Orbiter capacitance C_{orb} was set at 30 μF, which is a reasonable value given the works of Hawkins[21] and Liemohn.[22] The initial voltage applied to C_{orb} was set at the value to which the Orbiter was charged. Note that more recent work by Agüero[8] indicates that C_{orb} may have different charging and discharging capacitances. These results, however, do not affect our circuit model because we are dealing with very short, transient events and not the longer time responses of that work.

FPEG Model

The FPEG is modeled as a 100-mA, pulsed electron-current source with a 38.2-Hz pulse frequency, a 50% duty cycle, and 100-ns rise and fall times. It connects the Orbiter electrical ground and the ambient plasma medium represented in our model by Earth ground. In effect, when the FPEG current source is on, i.e., the FPEG is firing, it is able to simply dump charge because the source is not voltage dependent.

SETS Model

The configuration of the SETS experiment can be modeled for the present observations by the 35-MΩ internal impedance of its and DCORE's voltage monitors, indicated in Fig. 3 as R_{open}. Also modeled, but not shown in Fig. 3, is a 12-kHz double-pole RC low-pass filter that is part of the SETS measurement electronics. This filter was found to have only a minimal effect on the observations reported here.

Tether Reel Model

A simplified electrical model of the wound tether reel was developed on the basis of preflight tests.[13] This model, which has proven adequate for the analysis of electrical transients, is included in Fig. 3. The reel model was optimized to match responses seen with a fully loaded tether reel, including switching transient level and decay constant, capacitive discharge, and pulse response. It is a simple, two-section network that is valid for the present analysis because we need to consider only the primary reel resonance.

Electrodynamic Tether Model

The insulated, conducting tether is modeled as a coaxial transmission line using distributed lumped elements in a manner similar to that of Arnold and Dobrowolny,[23] Green et al.,[24] and Savich.[25] With this type of model, the outer conductor is formed by the ionospheric plasma, which is on the order of a Debye length away from the center conductor. James et al.[26] state that the tether, sheath, and surrounding plasma form an approximation to a coaxial rf transmission line to the degree that the surrounding plasma can be regarded as the outer conductor. This model consists of the standard resistance, inductance, capacitance, and conductance per unit length for coaxial lines (R, L, C, and G parameters) plus an additional E parameter, which represents the potential generated across each incremental length due to the tether's motion through the geomagnetic field.

Satellite Model

The satellite model is also based on a physical current source to model its interaction with the ionosphere. For the low tether currents achieved during TSS-1, the satellite can be considered as a spherical Langmuir probe with 0.8-m radius. The mathematical representation of the model, i.e., the I–V response $I_{sat}(V_{sat})$, is described in detail by Bilén et al.[4] and is similar to that used in the modified Orbiter model described earlier.

In addition to the physical current source at the satellite, there exists an effective nonlinear satellite-to-plasma capacitance, designated C_{sat}, which is dependent on satellite potential. This capacitance can be modeled as a concentric spherical capacitor, with the satellite as the inner conductor and the plasma as the outer conductor separated by the plasma sheath thickness.

Analysis

Computer simulations were performed using an analog circuit simulation software package similar to the standard Simulation Program with Integrated Circuit Emphasis (SPICE). These simulations were done by implementing the electrodynamic tether system model, described earlier and shown in Fig. 3, as a SPICE input deck and performing transient analyses on the circuit. By modeling the response of the TSS-1 system via computer simulation, we were able to determine the relevant importance of each section of the TSS system during its transient response from FPEG emission. In the present analysis, we were able to determine that the Orbiter–ionosphere interaction was the primary effect on the overall circuit and that the satellite and tether interaction had very little effect when TSS-1 was in its voltage mode and the FPEG was quickly modifying Orbiter potential by firing into the local ionosphere. The importance of the Orbiter–ionosphere interaction is to be expected because only microampere-level current flows through the tether in this mode, substantially reducing the effect of satellite–ionosphere interaction. This result is in contrast with what Bilén et al.[4] found when TSS-1 switched from its voltage to its current mode. In that case, the transient response was due primarily to the satellite–ionosphere interaction and the tether; the Orbiter effect was not significant.

Good qualitative agreement between the simulated and measured transients was found, in that the simulated transient voltage levels and ringing frequency matched the measured data within 10–20%. Figure 2 shows the comparison between the measured transients of the two observations and the simulated transients. Finding agreement between simulation and measurement allowed us to verify the TSS circuit model that we developed and gave us confidence in the parametric studies (described later) that we performed using the model.

There are several limitations of the electrodynamic tether system model as developed here that may affect the agreement between the computer simulations and the observations as well as the results of the parametric studies. First, several of the parameter values used in the current-source models are estimates rather than exact values because exact values are still the subject of active research. Specifically, the values for Orbiter effective collection areas and Orbiter capacitance are estimates taken from the literature. Second, the derivation of plasma density has some amount of uncertainty because of the temporal displacement between the CMM measurement in JFO2 step 2 and the tether current measurement made in JFO2 step 3, from which plasma density is calculated. Fortunately, because $n_e \propto 1/A_i$, any error in plasma density based on the estimate of Orbiter engine bell collection area is not compounded in the engine bell current source model because $I_{eng} \propto n_e A_i$. Third, the FPEG model is idealized because the simplifying assumption was made that 100 mA of electron current is always ejected into the local ionosphere when the FPEG is firing. This simplifying assumption may not always be valid because of filament efficiency. Fourth, this model is limited to low Orbiter charging levels because the voltage-dependent current source models used were developed for low charging levels. For conditions of higher positive and negative charging, the sources would need to be modified.[8]

Despite these limitations, our work shows that this simple circuit model can be used to accurately replicate, and hence also predict, transient spacecraft potential changes. We found that the Orbiter–ionosphere circuit, and specifically its current collection elements, was able to accurately model the magnitude of the transient spacecraft potential steps. Using our model, we performed parametric studies of the magnitude of spacecraft potential changes for varying plasma densities, FPEG currents, and electron collection areas. The results of these studies are shown in Figs. 4, 5, and 6, respectively. In each of these studies only one parameter was varied; the others were the same as in event 31 and were held constant. In each of these plots, model results are shown with the filled circles and the data point from event 31 is shown with the open square. Note that these studies are included to show the capabilities of a relatively simple model and to examine trends. Indeed, these studies do indicate high levels of charging that exceed the limits of the low-voltage Orbiter model.

In each of the parametric studies, the change in the spacecraft potential from floating potential as the FPEG is pulsed is measured.

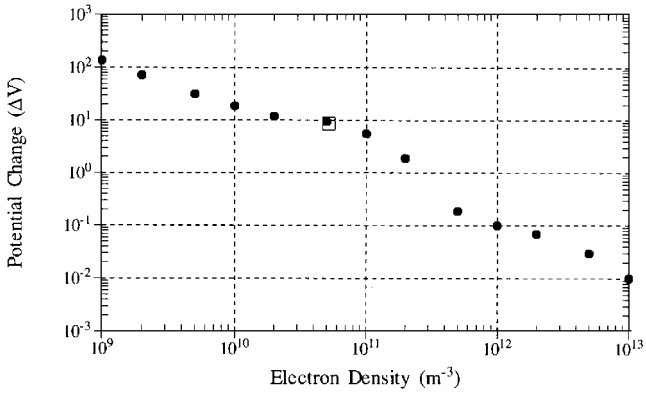

Fig. 4 Simulated spacecraft potential change due to FPEG pulsing as a function of plasma density (all other parameters are the same as event 31).

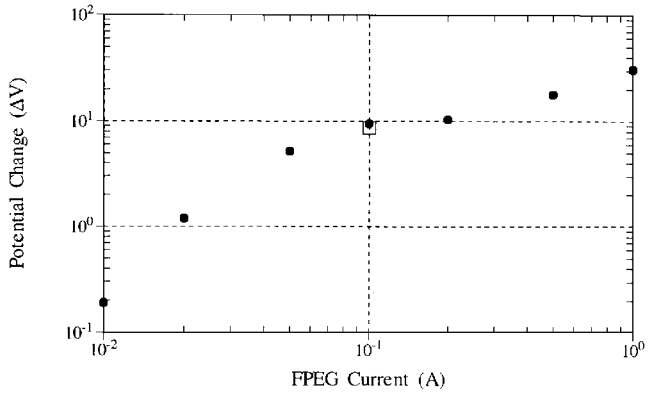

Fig. 5 Simulated spacecraft potential change due to FPEG pulsing as a function of FPEG current (all other parameters are the same as event 31).

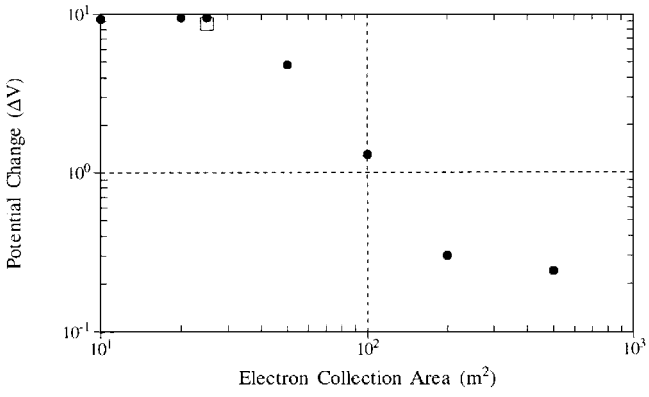

Fig. 6 Simulated spacecraft potential change due to FPEG pulsing as a function of electron collection area (all other parameters are the same as event 31).

In Fig. 4, we see that, as the plasma density n_e increases from a very low value ($\sim 10^9$ m^{-3}) to a high value ($\sim 10^{13}$ m^{-3}), the potential change drops from a very high value (>100 V) to an almost negligible amount (<0.01 V). This result indicates that in low densities the Orbiter could charge highly positive because of FPEG pulsing. In addition, the model predicts that the Orbiter transient charging due to FPEG pulsing would be greatly diminished if there is a locally enhanced electron flux. Note from this plot the expected transient charging levels for normal nighttime (low 10^{11} m^{-3}) and daytime (high 10^{11} m^{-3}) conditions. During nighttime, transient charging could be a few volts, whereas during daytime, only a few tenths of volts is expected. Figure 5 shows that the magnitude of the FPEG discharge current I_{FPEG} also affects the magnitude of the potential change, increasing the magnitude as the current increases. Increasing the electron and ion collection areas A_e and A_i, as shown in Fig. 6, reduces the magnitude of the potential change. Although these results are to be expected, they do show the importance of our model in predicting transient spacecraft potential changes.

In a manner similar to that presented here, circuit models of the interaction of other spacecraft, in particular large spacecraft, with the ionosphere can be developed. In developing these models, it is extremely important not only to use proper current sources to model the spacecraft–plasma interaction but also to identify any spacecraft subsystems that may be affected by potential changes and other spacecraft–plasma interactions. For example, the pulse response of the TSS tether reel subsystem elicited by the rapidly changing Orbiter potential provided up to a factor of 1.6 times the step voltage, e.g., a 10-V change in Orbiter potential could result in 16-V peak voltage across the system.

Summary

The electrical transient response of TSS due to the firing of an electron generator into the ionosphere has been investigated experimentally and by computer-based circuit simulations. Because of the low density of the surrounding ionospheric plasma, the FPEG was able to quickly modify the potential of the Shuttle Orbiter. The resulting voltage transients were measured by the SETS experiment, which could selectively sample the system voltage in high-speed bursts. The computer simulation shows that the electrical transient response of the system is due to a combination of both the TSS electrical circuit and the modification of the Shuttle potential due to the FPEG firing into the surrounding ionospheric plasma. The computer model has proven successful at replicating the Orbiter transient voltage response for the conditions experienced during TSS-1. In addition, we were able to determine that, when TSS-1 was in its voltage mode and the FPEG was quickly modifying Orbiter potential by firing into the local ionosphere, 1) the Orbiter–ionosphere interaction was the primary effect on the overall circuit and 2) the satellite and tether interaction had very little effect. Using our model, we performed parametric studies of the magnitude of spacecraft potential changes for varying plasma densities, FPEG currents, and electron collection areas.

The results presented here have implications for the use of electron generators that actively modify the potential of their host spacecraft. These implications are based on an understanding of the physical interaction of TSS with the surrounding ionospheric plasma. For the TSS-1 case in which the tether system was in its voltage mode and the FPEG was firing into a local ionosphere region of low plasma density, the voltage transient response was driven primarily by the I–V response of the Orbiter and the second-order underdamped response of the tether reel circuit. If the tether reel were to be replaced with a different circuit, however, the ionospheric effects described here would still be present, i.e., the magnitude of the spacecraft potential changes. From our results, we have shown that transients can be caused not only by switching of currents in a tethered system but also by electron emissions from one of the end points that quickly modify its potential.

Acknowledgments

One of the authors (S.G.B.) would like to thank NASA for providing him with a Graduate Student Researchers Program Fellowship to perform this research. This work was also done under NASA Contract NAS8-93831. The SPICE software package used in this research is HSPICE (version H93A) developed by Meta-Software, Inc. We wish to thank the entire SETS TSS-1 mission team, which contributed to obtaining this data set under very difficult conditions.

References

[1] Garrett, H. B., and Whittlesey, A. C., "Spacecraft Charging, An Update," AIAA Paper 96-0143, Jan. 1996.

[2] Hastings, D. E., "A Review of Plasma Interactions with Spacecraft in Low Earth Orbit," *Journal of Geophysical Research*, Vol. 100, No. A8, 1995, pp. 14,457–14,483.

[3] Dobrowolny, M., and Melchioni, E., "Electrodynamic Aspects of the First Tethered Satellite System," *Journal of Geophysical Research*, Vol. 98, No. A8, 1993, pp. 13,761–13,778.

[4] Bilén, S. G., Gilchrist, B. E., Bonifazi, C., and Melchioni, E., "Transient Response of an Electrodynamic Tether System in the Ionosphere: TSS-1 First Results," *Radio Science*, Vol. 30, No. 5, 1995, pp. 1519–1535.

[5]Kawashima, N., Sasaki, S., Oyama, K. I., Hirao, K., Obayashi, T., Raitt, W. J., White, A. B., Williamson, P. R., Banks, P. M., and Sharp, W. F., "Results from a Tethered Rocket Experiment (CHARGE-2)," *Advances in Space Research*, Vol. 8, No. 1, 1988, pp. 197–201.

[6]Allred, D. B., Benson, J. D., Cohen, H. A., Raitt, W. J., Burt, D. A., Katz, I., Jongeward, G. A., Antoniades, J., Alport, M., Boyd, D., Nunnally, W. C., Dillon, W., Pickett, J., and Torbert, R. B., "The SPEAR-1 Experiment: High Voltage Effects on Space Charging in the Ionosphere," *IEEE Transactions on Nuclear Science*, Vol. 35, No. 6, 1988, pp. 1386–1393.

[7]Raitt, W. J., Myers, N., Roberts, J., Thompson, D., Gilchrist, B., and Sasaki, S., "Recent Observations of High Voltage Spacecraft–Environment Interaction at LEO Altitudes Using Sounding Rockets," AIAA Paper 90-0635, Jan. 1990.

[8]Agüero, V., "A Study of Electrical Charging on Large LEO Spacecraft Using a Tethered Satellite as a Remote Plasma Reference," Ph.D. Thesis, Dept. of Aeronautical and Astronautical Engineering, Stanford Univ., Stanford, CA, 1996.

[9]Dobrowolny, M., and Stone, N. H., "A Technical Overview of TSS-1: The First Tethered Satellite System Mission," *Il Nuovo Cimento della società italiana di fisica*, Vol. 17C, No. 1, 1994, pp. 1–12.

[10]Agüero, V., Banks, P. M., Gilchrist, B., Linscott, I., Raitt, W. J., Thompson, D., Tolat, V., White, A. B., Williams, S., and Williamson, P. R., "The Shuttle Electrodynamic Tether System (SETS) on TSS-1," *Il Nuovo Cimento della società italiana di fisica*, Vol. 17C, No. 1, 1994, pp. 49–65.

[11]Banks, P. M., Raitt, W. J., White, A. B., Bush, R. I., and Williamson, P. R., "Results from the Vehicle Charging and Potential Experiment on STS-3," *Journal of Spacecraft and Rockets*, Vol. 24, No. 2, 1987, pp. 138–149.

[12]*Tethered Satellite System (TSS) Data Reference Book*, 1st ed., Civil and Space Communications, Martin Marietta, Denver, CO, 1992, pp. 44–54.

[13]Bilén, S. G., Lauben, D. S., Williamson, P. R., Williams, S. D., Agüero, V. M., and Gilchrist, B. E., "Electrical Characterization of the TSS-1 and TSS-1R Tether Deployer System," Space Physics Research Lab., Rept. 057-0199, Univ. of Michigan, Ann Arbor, MI, Aug. 1994.

[14]Grossner, N. R., *Transformers for Electric Circuits*, 2nd ed., McGraw–Hill, New York, 1983, pp. 362–419.

[15]Thompson, D. C., Raitt, W. J., Bonifazi, C., Williams, S. D., Agüero, V. M., Gilchrist, B. E., and Banks, P. M., "TSS-1: Orbiter Current and Voltage Experiments," AIAA Paper 93-0702, Jan. 1993.

[16]Oberhardt, M. R., Hardy, D. A., Thompson, D. C., Raitt, W. J., Melchioni, E., Bonifazi, C., and Gough, M. P., "Positive Spacecraft Charging as Measured by the Shuttle Potential and Return Electron Experiment," *IEEE Transactions on Nuclear Science*, Vol. 40, No. 6, 1993, pp. 1532–1541.

[17]Oberhardt, M. R., Hardy, D. A., Slutter, W. E., McGarity, J. O., Sperry, D. J., Everest, A, W., III, Huber, A. C., Pantazis, J. A., and Gough, M. P., "The Shuttle Potential and Return Electron Experiment (SPREE)," *Il Nuovo Cimento della società italiana di fisica*, Vol. 17C, No. 1, 1994, pp. 67–83.

[18]Brundin, C. L., "Effects of Charged Particles on the Motion of an Earth Satellite," *AIAA Journal*, Vol. 1, No. 11, 1963, pp. 2529–2538.

[19]Garrett, H. B., "The Charging of Spacecraft Surfaces," *Journal of Geophysics and Space Physics*, Vol. 19, No. 4, 1981, pp. 577–616.

[20]Thompson, D. C., Raitt, W. J., Oberhardt, M. R., Hardy, D. A., Agüero, V. M., Linscott, I. R., Neubert, T., Gilchrist, B. E., and Banks, P. M., "Global Survey of TSS-1 Current Collection as Measured by the SETS Experiment (Abstract)," *EOS Transactions AGU*, Vol. 73, No. 43, Fall Meeting Supplement, 1992, p. 422.

[21]Hawkins, J. G., "Vehicle Charging and Return Current Measurements During Electron Beam Emission Experiments from the Shuttle Orbiter," Ph.D. Thesis, Dept. of Electrical Engineering, Stanford Univ., Stanford, CA, April 1988.

[22]Liemohn, H. B., "Electrical Charging of Shuttle Orbiter," *IEEE Transactions on Plasma Science*, Vol. PS-4, No. 4, 1976, pp. 229–240.

[23]Arnold, D. A., and Dobrowolny, M., "Transmission Line Model of the Interaction of a Long Metal Wire with the Ionosphere," *Radio Science*, Vol. 15, No. 6, 1980, pp. 1149–1161.

[24]Greene, M., Wheelock, D., and Baginski, M., "Electrodynamics of the Getaway Tether Experiment," *Journal of Spacecraft and Rockets*, Vol. 26, No. 6, 1989, pp. 452–459.

[25]Savich, N. A., "Electrodynamics of Tethered Satellite Systems: Two Concepts," 40th Congress of the International Astronautical Federation, Paper IAF-89-013, Málaga, Spain, Oct. 1989.

[26]James, H. G., Balmain, K. G., Bantin, C. C., and Hulbert, G. W., "Sheath Waves Observed on OEDIPUS A," *Radio Science*, Vol. 30, No. 1, 1995, pp. 57–73.

A. C. Tribble
Associate Editor